Distinct pattern of inflammation in bronchoalveolar lavage and bronchial mucosa of children with cystic fibrosis

Online Repository

Nicolas Regamey[1,2,3]; Lemonia Tsartsali[1]; Tom N Hilliard[12]; Oliver Fuchs[3]; Huileng Tan[1,2]; Jie Zhu[2]; Yu-Sheng Qiu[2]; Eric WFW Alton[2]; Peter K Jeffery[2]; Andrew Bush[1]; Jane C Davies[1,2]

[1]Department of Paediatric Respiratory Medicine, Royal Brompton Hospital, Sydney Street, London SW3 6NP, United Kingdom

[2]Department of Gene Therapy, National Heart and Lung Institute, Imperial College London, Manresa Road, London SW3 6LR, United Kingdom

[3]Division of Paediatric Respiratory Medicine, Department of Paediatrics, University Hospital of Bern, 3010 Inselspital Bern, Switzerland

METHODS

Subjects - CF children

All CF children undergoing flexible bronchoscopy for a clinical reason at the Royal Brompton Hospital between March 2003 and June 2007 (n= 183) were considered for participation in the study. One-hundred and seven CF children were recruited. Sufficient biopsy material (see inclusion criteria below) was available in 46 of them. These children had following CFFTR genotypes: F508del/F508del (n=27, 59%); F508del/G542X (n=2, 4%); F508del/1717-1G>A (n=2; 4%); F508del/other (n=6, 13%); other or unknown (n=9, 20%). CF diagnoses had been made clinically, as CF newborn screening had not been implemented at the time of this study.

Flexible bronchoscopy

Depending on the size of the child, different bronchoscopes were used: BFXP40 (2.8 mm external diameter), BF-3C20 or 3C40 (3.6 mm external diameter), or BF-MP60 (videobronchoscope, 4.0 mm external diameter), or BF-P20D (4.9 mm external diameter), all from Olympus (Tokyo, Japan). Up to 5 endobronchial biopsies were taken under direct vision from a standardized site (i.e. sub-segmental bronchi of the right lower lobe). Small reusable forceps (FB-56D, oval cup with rat tooth jaw; KeyMEd; Southend-on-Sea, Essex, UK) were used with the 2.8-mm or 3.6-mm bronchoscope (both with a 1.2-mm working channel). Large reusable forceps (FB-19-C1, oval cup standard; KeyMed) or single use forceps (FB-231D, oval cup standard; KeyMed) were used with the 4.0-mm or 4.9-mm bronchoscope (working channel 2.0 vs. 2.2 mm, respectively).

Bronchoalveolar lavage (BAL)

BAL was performed for clinical reasons in all children, and was primarily used for microbiological assessment. Therefore, in some cases, there was not enough material left for cell counts.

Biopsy processing and staining

Biopsies were fixed in 10% formal saline solution overnight and processed into paraffin blocks. One 3 μm section was stained with haematoxylin and eosin and categorized as ‘evaluable` or ‘non-evaluable’. To be categorized as “evaluable”, a biopsy had to fulfill following criteria: (i) presence of epithelium, reticular basement membrane (RBM) and

subepithelial tissue; (ii) good orientation; (iii) minimal crush, edema or blood within the biopsy (E1). Biopsies with 'evaluable' sections were then cut further and up to ten 3 μm sections were then taken at 50 μm intervals and stained with monoclonal mouse anti-human neutrophil elastase (NE)(M0752, DAKO, Glostrup, Denmark) for neutrophils, polyclonal rabbit anti-human CD3 (A0452, DAKO, Glostrup, Denmark) for T-lymphocytes, monoclonal mouse anti-human CD20cy (M0755, DAKO, Glostrup, Denmark) for B-lymphocytes, monoclonal mouse anti-human CD68 (M0876, DAKO, Glostrup, Denmark) for macrophages, monoclonal mouse anti-human eosinophilic cationic protein (EG2)(Pharmacia & Upjohn Diagnostics AB, Uppsala, Sweden) for eosinophils and monoclonal anti-tryptase (M7052, DAKO, Glostrup, Denmark) for mast cells (E2-E4). Neutrophils, T- and B-lymphocytes and macrophages were identified using the DAKO Autostainer streptavidin method® (DAKO, Glostrup, Denmark) after heat-mediated antigen retrieval by pressure cooking in 0.01M citrate buffer (except for neutrophils, for which no pre-treatment was needed). Eosinophils and mast cells were identified using the EnVision-alkaline phosphatase (EV-AP) technique (DAKO, Glostrup, Denmark), as previously described (E5). Some biopsies did not yield enough sections to perform all stains.

A subset of the biopsies (n=30) from CF children was also stained with monoclonal mouse anti-human CD83 (VP-C368, Vector, Burlingame, Ca, USA) for mature dendritic cells (DCs), as previously described (E6). However, there were only very few positive cells in these samples (1-2 positive cells in only 3/30 biopsy samples), and therefore this stain was not performed for the rest of the biopsy samples.

Quantification of inflammatory cells on biopsies

Sections were coded and counted by two blinded observers (NR and LT). Areas of subepithelial tissue, excluding areas with mucus-secreting glands, bronchial smooth muscle and large vessels, were assessed using an Apple Macintosh computer and Image 1.5 software (Apple Computer, Cupertino, CA). To be included in the study, we required *a priori* that each child had at least one biopsy with at least 0.1 mm^2 of subepithelial tissue (E7).

Using a light microscope (Dialux 20, Leitz, Wetzlar, Germany) at x400 magnification, area profile counts were used to count inflammatory cells in the subepithelial tissue of each biopsy specimen. The data were expressed as the number of cut cell profiles with a nucleus visible (i.e., positive cells) per square millimeter of the subepithelium, the mean of all evaluable biopsy specimens representing the value for that subject.

Repeatability and variability

Intra-observer repeatability and within-observer, within-biopsy and between-biopsy variability were determined (E8). The mean intra-observer repeatability, expressed as coefficient of variation (C%V) for cell count measurements on four occasions ranged from 17.7% (T-lymphocytes) to 23.9% (B-lymphocytes, Table E1).

Table E1. Repeatability and variability of cell count measurements, expressed as percent coefficient of variation (CV).

	Neutrophils	T-lymphocytes	B-lymphocytes	Macrophages	Mast cells	Eosinophils
Intra-observer repeatability	13.4	7.7	23.9	14.9	9.1	8.1
Within-biopsy variability	21.9	9.3	33.9	13.2	12.9	n.a.
Between-biopsy variability	130.2	64.2	51.5	63.8	76.9	173.2

Definition of abbreviation: n.a. = not assessed

Within a single biopsy, the between-section CV for four sections ranged from 9.3% (T-lymphocytes) to 33.9% (B-lymphocytes). Between-biopsy CV ranged from 51.5% (B-lymphocytes) to 173.2% (eosinophils). Overall inter-observer agreement of the two blinded observers (NR and LT) for cell counts was good (ICC=0.87) and ranged from 0.61 (neutrophils) to 0.95 (mast cells). These results are similar to those previously published (E9).

Reticular basement membrane (RBM) thickness

Reticular basement membrane (RBM) thickness was measured on 3 μm thick haematoxylin and eosin-stained coded sections as previously described (E10, E11). One section of each biopsy was selected which showed identifiable epithelium and submucosal with at least 800 μm of RBM. RBM thickness was measured by a blinded observer (NR) using light microscopy and computer-aided image analysis (NIH Image 1.55; National Institutes of Health, Bethesda, Maryland, USA) by taking the geometric mean of 40 measurements at 20 μm intervals. The mean intra-observer repeatability as coefficient of variation (CV) for RBM thickness measurements on four occasions was 5.2%. Within a single biopsy, the between-

section CV for seven sections was 18.9%. The mean [SD] between-biopsy CV obtained from 10 patients in whom RBM thickness was measured in 3 biopsies was 15.8 [6.6]%.

Airway smooth muscle (ASM) mass

Airway smooth muscle (ASM) mass was assessed on 3 μm thick haematoxylin and eosin stained sections using equations from design-based stereology (E12, E13), as described previously (E14). The ASM volume fraction was measured using point and line intersection counting. Briefly, the numbers of points overlying ASM and other subepithelial tissue and the number of lines intersecting the apical surface of RBM by light microscopy were recorded using a x10 lens and a M168 counting grid (x390 total magnification, Figure E3).

Stereological data were calculated from point and line intersection counts as follows:

(1) volume fraction of ASM indexed to volume of subepithelial tissue: Vv (sm/subepithelium) = (Σ points on ASM) / (Σ points on subepithelial tissue)

(2) volume fraction of ASM indexed to surface area of RBM: V/S (sm/rbm) = (Σ points on ASM x l(p)) / (2 x Σ line intersections with RBM); where l(p) denotes length per point (μm)

Statistical analysis

Data were analyzed on a ‘per individual’ as opposed to ‘per biopsy’ basis, e.g. the sum of the measurements obtained from all biopsies of a given subject was taken as value for this subject. SPSS v15 (SPSS Inc, Chicago, IL, USA) and Stata IC 11.0 for Windows (StataCorp, College Station, TX, USA) were used for statistical analysis.

Linear regression

Having found a positive association of inflammatory cell counts with age within the CF group, we performed multivariable regression analyses to adjust group differences for age for all subsequent analyses done within the CF group. Multivariable models were fitted with parameters significantly associated with outcomes (numbers of inflammatory cells) in univariable models (i.e. presence of chest exacerbation, presence of *Aspergillus sp.* and presence of *Pseudomonas aeruginosa* in BAL). We tested whether these parameters remained significantly associated with outcomes after a backward stepwise exclusion strategy of dropping the explanatory variable with the highest p-value until only significant associations

were left in the final model. A p-value <0.05 was considered significant. For linear regression analyses, non-normally distributed cell counts were transformed to normalize their distribution (log-transformation for total cell counts, neutrophils and macrophages in BAL and total cell counts in biopsies; square-root transformation for lymphocytes and eosinophils in BAL and for neutrophils, macrophages, lymphocytes and eosinophils in biopsies).

REFERENCES

E1. Regamey N., Hilliard TN, Saglani S, Zhu J, Scallan M, Balfour-Lynn IA, Rosenthal M, Jeffery PK, Alton EW, Bush A, and Davies JC. Quality, size, and composition of pediatric endobronchial biopsies in cystic fibrosis. *Chest* 2007; 131(6):1710-7.

E2. O'Shaughnessy TC, Ansari TW, Barnes NC et al. Inflammation in bronchial biopsies of subjects with chronic bronchitis: inverse relationship of CD8+ T lymphocytes with FEV1. Am J Respir Crit Care Med 1997; 155:852-857

E3. Zhu J, Qiu YS, Majumdar S et al. Exacerbations of Bronchitis: bronchial eosinophilia and gene expression for interleukin-4, interleukin-5, and eosinophil chemoattractants. Am J Respir Crit Care Med 2001; 164:109-116.

E4. Qiu Y, Zhu J, Bandi V et al. Biopsy neutrophilia, neutrophil chemokine and receptor gene expression in severe exacerbations of chronic obstructive pulmonary disease. Am J Respir Crit Care Med 2003; 168:968-975.

E5. Gamble E, Grootendorst DC, Brightling CE, Troy S, Qiu Y, Zhu J, Parker D, Matin D, Majumdar S, Vignola AM, et al. Antiinflammatory effects of the phosphodiesterase-4 inhibitor cilomilast (ariflo) in chronic obstructive pulmonary disease. *Am J Respir Crit Care Med* 2003; 168:976-982.

E6. Tsoumakidou M, Elston W, Zhu J, Wang Z, Gamble E, Siafakas NM, Barnes NC, Jeffery PK. Cigarette smoking alters bronchial mucosal immunity in asthma. *Am J Respir Crit Care Med.* 2007;175:919-25

E7. Barbato A, Turato G, Baraldo S, Bazzan E, Calabrese F, Panizzolo C, Zanin ME, Zuin R, Maestrelli P, Fabbri LM, et al. Epithelial damage and angiogenesis in the airways of children with asthma. *Am J Respir Crit Care Med* 2006;174:975-981.

E8. Sont JK, Willems LN, Evertse CE, Hooijer R, Sterk PJ, van Krieken JH. Repeatability of measures of inflammatory cell number in bronchial biopsies in atopic asthma. *Eur Respir J* 1997;10:2602-2608.

E9. Sont JK, Willems LN, Evertse CE, Hooijer R, Sterk PJ, van Krieken JH: Repeatability of measures of inflammatory cell number in bronchial biopsies in atopic asthma. Eur Respir J 1997;10:2602-2608.

E10. Hilliard TN, Regamey N, Shute JK, Nicholson AG, Alton EW, Bush A, Davies JC. Airway remodelling in children with cystic fibrosis. *Thorax* 2007;62:1074-1080.

185E11. Sullivan P, Stephens D, Ansari T, Costello J, Jeffery P. Variation in the measurements
186 of basement membrane thickness and inflammatory cell number in bronchial biopsies.
187 *Eur Respir J* 1998;12:811-815.
188E12. Weibel, E. R., C. C. Hsia, and M. Ochs. 2007. How much is there really? Why
189 stereology is essential in lung morphometry. *J Appl Physiol* 102(1):459-67.
190E13. Ochs, M. 2006. A brief update on lung stereology. *J Microsc* 222(Pt 3):188-200.
191E14. Regamey N, Ochs M, Hilliard TN, Muhlfeld C, Cornish N, Fleming L, Saglani S,
192 Alton EW, Bush A, Jeffery PK, et al. Increased airway smooth muscle mass in
193 children with asthma, cystic fibrosis, and non-cystic fibrosis bronchiectasis. *Am J*
194 *Respir Crit Care Med* 2008;177:837-843

LEGENDS TO THE SUPPLEMENTAL FIGURES

Figure E1. Reticular basement membrane (RBM) thickness in biopsies obtained from cystic fibrosis (CF) children (n=46) and controls (n=16). RBM was significantly thicker in the CF group. Horizontal bars represent means.

Figure E2. Panel A: Relationship between reticular basement membrane (RBM) thickness in biopsies obtained from cystic fibrosis (CF) children (n=46) and age. Panel B: Relationship between reticular basement membrane (RBM) thickness in biopsies obtained from control children (n=16) and age.

Figure E3. Representative low power view (x200) of an endobronchial biopsy section stained with haematoxylin and eosin with superimposition of a M168 counting grid, allowing the measurement of ASM volume fraction

Figure E4. Airway smooth muscle (ASM) content in endobronchial biopsies from children with cystic fibrosis (CF, n=46) compared to control children (n=16). *Definition of abbreviations*: Vv (sm/subepithelium) = volume fraction of ASM indexed to volume of airway subepithelial tissue. Horizontal bars represent medians.

215**Figure E1**

216

217

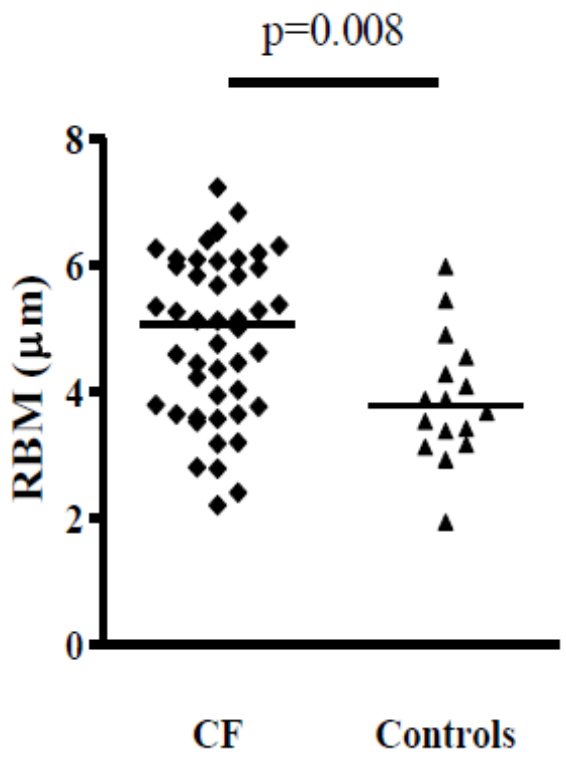

218

219**Figure E2**

220

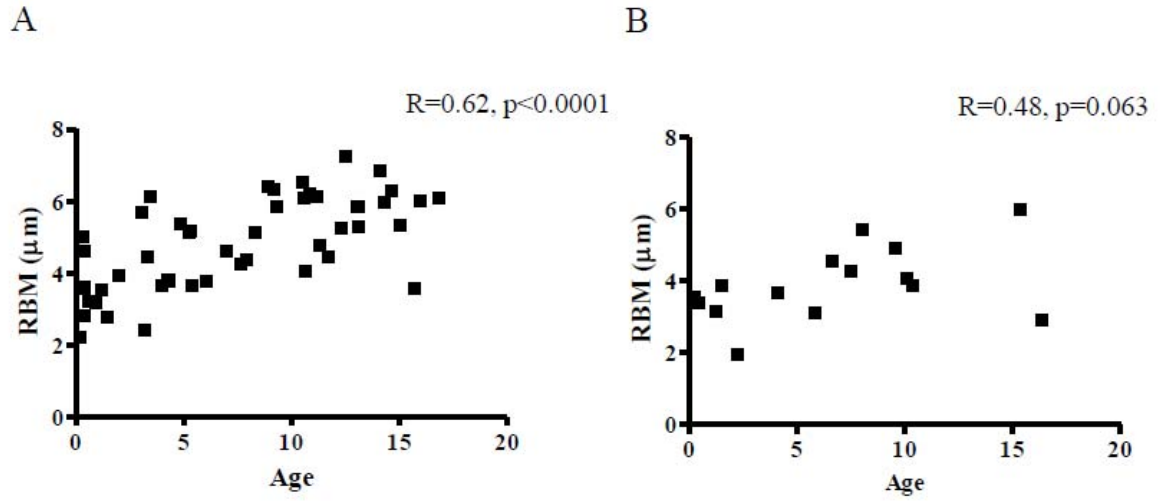

221

222**Figure E3**

223

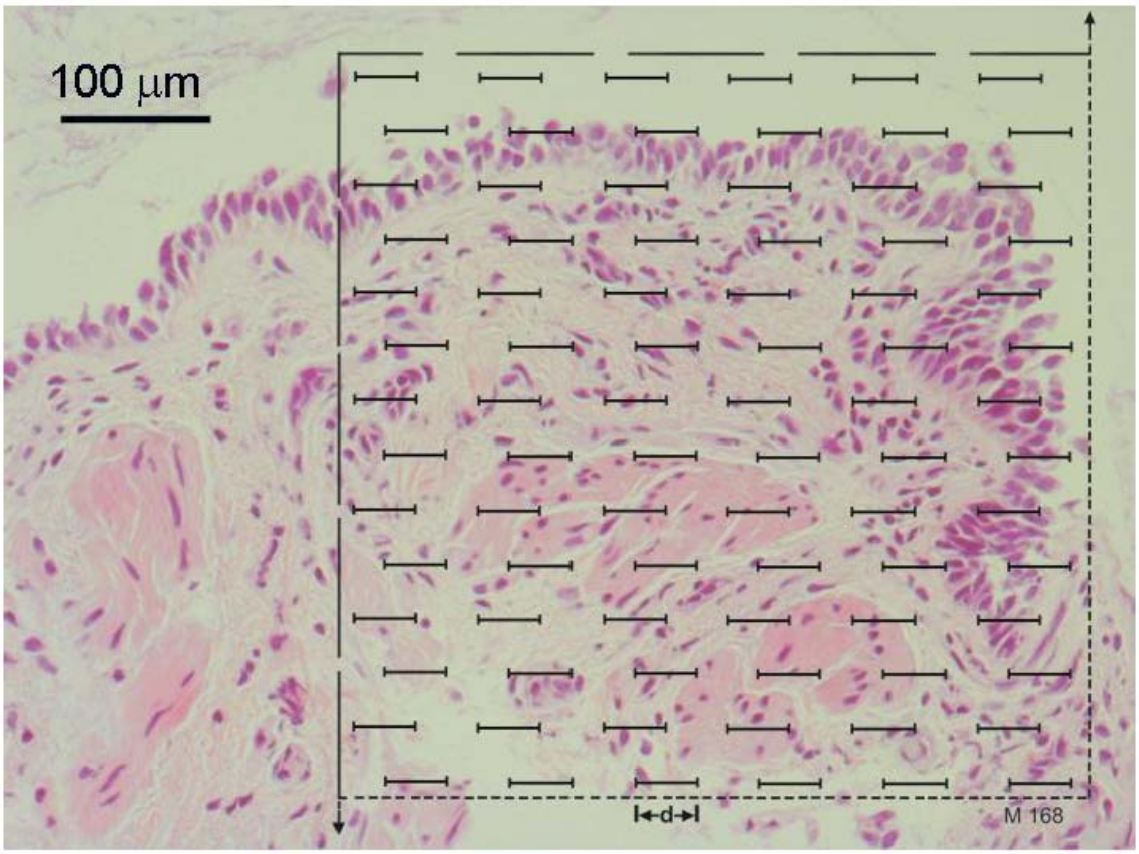

224

225**Figure E4**

226

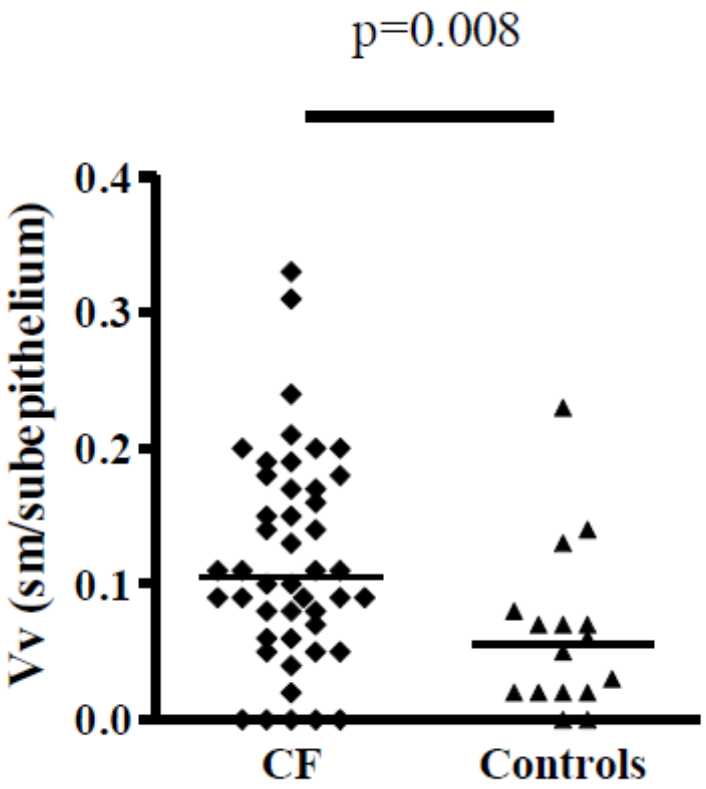

227